ELEVATION-CONTROLLED BLOCK ADJUSTMENT FOR WEAKLY CONVERGENT SATELLITE IMAGES

Liang-Chien Chen *, Tee-Ann Teo, and Chao-Yuan Lo

Center for Space and Remote Sensing Research, National Central University, Jhongli, Taoyuan 32001, Taiwan, China-(lcchen, ann, freezer)@csrsr.ncu.edu.tw

Commission I, WG I/5

KEY WORDS: Orientation, orthorectification, georeferencing, bundle adjustment, rational function model.

ABSTRACT:

In order to acquire the largest possible coverage for environmental monitoring, small overlapping for satellite images is often the case. Hence, the traditional 3-D bundle adjustment as used in photogrammetry may not be directly employed for orientation modeling. In this investigation, we compare three approaches of block adjustment methods for satellite images that are with weak convergent geometry by using Digital Elevation Model (DEM) as an elevation control. The first one is a revised version of traditional bundle adjustment. The second one is based on the direct georeferencing approach. The third one is a rational function model (RFM) with sensor-oriented rational polynomial coefficients (RPC). These approaches integrate the collocation technique to improve the positioning accuracy. In the bundle adjustment, we calculate the orientation parameters by using the collinearity equations. Meanwhile, the DEM is used as an elevation control. Then, we collocate the orientation parameters by using least squares filtering. For the direct georeferencing, we adjust the orientation parameters from the satellite's ephemeris data, then, we calculate the error vectors for each tie point using DEM and refine the orientation parameters using the least squares filtering. In the implementation of elevation control in RFM, the block adjustment deals with the coordinate transformation and the observation equations of 3-D ground coordinates. In the adjustment, an iterative procedure is employed to combine the adjustment with DEM elevation control. The experimental results indicate that the proposed method using DEM as elevation control could significantly improve the geometric accuracy as well as the geometric discrepancies.

1. INTRODUCTION

1.1 Motivation and Goals

One of the most important applications of satellite images is the landuse/landcover monitoring. It is often the case that the area of interest covers two or more images. Thus, the mosaicking becomes a must. Another prominent application using the remotely sensed images is change detection. In that case, multi-temporal images should be registered before performing the detection. To enhance the quality of geometric registration in both cases, the simultaneous block adjustment is preferable. Thus, the adjusted orientation parameters could provide a sound fundamental for rigorous orthorectification.

1.2 Related Works

The approaches of the orientation modeling may be categorized in three types, namely, direct georeferencing(Downman and Michalis, 2003; Poli et al., 2004), bundle adjustment (Westin, 1990; Chen and Lee, 1993; Orun and Natarajan, 1994; Toutin, 2003), and the rational function model (Grodecki and Dial, 2003; Fraser et al., 2006). From photogrammetric point of view, 3D bundle adjustment is the most mature approach that the collinearity condition for all of the tie points and ground control points (GCPs) are satisfied simultaneously. However, due to satellites' small field of view, the favourable convergent geometry could not be always expected. In addition, the overlapping area between satellite strips would not be always large enough. Hence, the bundle adjustment should be modified to adopt for the weakly convergent geometry.

Direct georeferencing, on the other hand, could reduce the required number of GCPs. However, to keep the accuracy of the image parts within the overlapping area of connecting strips, tie points should be included. Again, some improvements should be added to cope with the weakly convergent geometry or small overlapping areas. Due to its simple implementation and standardization, the RFM have been widely used in the remote sensing society. To some extent, the RFM may be interpreted as another form of direct georeferencing when rational polynomial coefficients are derived from GPS, INS, and star tracker. For some high resolution satellite images, IKONOS for instance, RPCs are provided rather than the original orientation parameters. Thus, the same problem occurs again for the image blocks with weak convergent geometry.

1.3 The Need for More Investigation

Different from area sensors, the linear array sensors that are used in the imaging systems for high resolution satellite cannot satisfy the demands of large coverage and stereoscopic observation at the same time. In reality, the major applications of the remote sensing images are the detection of natural resources and the monitoring for geo-environment. In order to acquire the largest possible coverage, the overlapping area of satellite images is small in many cases. Thus, the weak geometry of intersection will cause large elevation error. In

* Corresponding author.

other words, the base-to-height ratio of multi-orbit satellite images is, frequently, not large enough.

1.4 The Purposed Method

The objective of this investigation is to propose a solution to solve the problem of weakly convergent geometry for satellite image blocks. Three types of the orientation modeling including direct georeferencing, bundle adjustment, and RFM are given. To provide the solution, a digital elevation model is assumed available. Since the final goal is to produce orthoimages instead of 3-D surface reconstruction, the assumption of the availability of DEM is justified. To compensate for the local systematic errors, least squares collocation is integrated in the solution.

In the ***direct georeferencing***, the observation vectors for GCPs and tie points are formulated first. By employing a preliminary fitting of the orbit parameters, all of the discrepancies for GCPs and the parallaxes for tie points are calculated. Then the discrepancy/parallax vectors are employed in a least squares collocation.

In the ***modified bundle adjustment***, traditionally, three groups of the observation equations including image coordinates with collinearity condition, orientation parameters, and ground coordinates are employed as the fundamental. Then, an elevation-controlled mechanism is proposed by using a DEM. The mechanism is done in such a way that the ground coordinates are iterated by simultaneously satisfying the collinearity condition, the ground surface, and the weighted orientation parameters. Finally, a least squares collocation is included to adjust for the local systematic errors.

In the implementation of elevation control in ***rational function model***, a typical block adjustment is developed first. Since the RPCs are derived from precision GPS, INS, and star tracker, we treat it as constants. Thus, the block adjustment deals with the affine transformation and the observation equations of 3-D ground coordinates. In the adjustment, DEM is used as an elevation control. The ground coordinates are iterated to satisfy the RFM, ground surface, and the weighted ground coordinates simultaneously. Again, a least squares collocation may also be included.

2. METHODOLOGY

The proposed scheme comprises three block adjustments models: (1) the direct georeferencing model, (2) the modified bundle adjustment, and (3) the rational function model. The detail for each model is given as follows.

2.1 Direct Georeferencing

The direct georeferencing model comprises two major parts. The first part is the preliminary orbit fitting by using the GCPs. The second one is to refine the orbit by using the least squares collocation with tie points. A DEM is used to be an elevation control in the block adjustment procedure.

The satellite on-board ephemeris data include orbital parameters and attitude data. We use the data to establish the state vectors of satellite position and the light-of-sight. The state vectors are illustrated in Figure 1. The collinearity condition equation of state vectors is shown as equation (1). Once those exterior orientation parameters are modeled, the corresponding ground coordinates for an image pixel can be calculated. We use the GCPs to adjust the orbital parameters. Equation (2) shows the collinearity equation with preliminary orbit fitting. In order to compensate the error for orbital parameters, a low degree polynomial is applied in this state,

$$\vec{G} - \vec{P} = S\vec{U} \quad (1)$$

$$\vec{G} - (\vec{P} + \Delta\vec{P}_t) = S\vec{U} \quad (2)$$

where,

G is the ground point vector,
P is the satellite position vector,
U is the satellite light-of-sight vector,
S is the scale factor, and
ΔP is the orbital polynomial function.

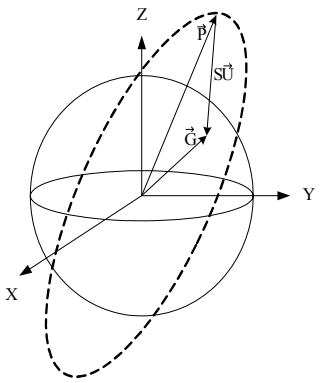

Figure 1. Illustration of State vectors

In the process of images stitching, we use the residual vectors on tie points to collocate the discrepancy of images. So we need to compute the residual vectors for tie points. First we use the orbit parameters and the image coordinates of a tie point to calculate the observation vector. Given a DEM, the ray tracing technique is applied to determine the ground position of a tie point. The procedure is repeated for its counterpart in the other image. Referring to Figure 2, a pair of tie point has two ground corresponding points. It means the discrepancy between the images. The middle of two ground points are used as a constraint. The residual vector on each tie point is the vector from one ground position to the middle of the two points.

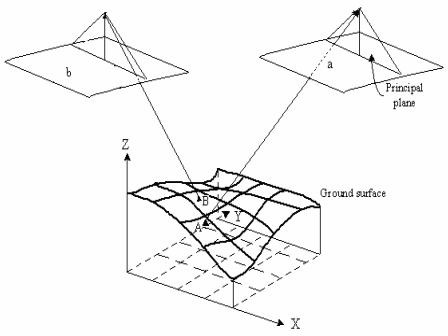

Figure 2. Illustration of error vector on tie point

The discrepancy vectors of tie points are employed in a least squares collocation for block adjustment. By doing so, we assume that the x, y, z-axis are independent. Three one-dimensional functions are applied to adjust the orbit. The model of least squares filtering (Mikhail and Ackermann, 1982) is shown as equation (3),

$$S_k = \sigma_k \bullet \Sigma_k^{-1} \bullet l_k \tag{3}$$

where,

k is x,y,z axis

S_k is the correction value of the interpolating point,

σ_k is the row covariance matrix of the interpolating point with respect to tie points,

Σ_k is the covariance matrix for tie points, and

l_k is the residual vectors for tie points.

2.2 Modified Bundle Adjustment

The modified bundle adjustment also comprises two major parts. The first one is to define a Working Coordinate System for bundle adjustment. The second part is the bundle adjustment using DEM as an elevation control.

Before performing the bundle adjustment, we should transform all of the geometric parameters into a same coordinate system, including orientation parameters, GCPs, and tie points. Hence, we define a Work Coordinate Systems with coordinate direction of LVLH (Local Vertical Local Horizontal). The origin is set at the centroid of GCPs. We may, thus, avoid numerical instability and the projection error caused by a long track. In addition, the high correlation between orbit parameters and attitudes can be better depicted and separated in weighting.

The collinearity condition equations state that the exposure station, any object points, and its image point all lie along a straight line. The equations are modified, as shown in equation 4, to fit the imaging geometry of satellite images. The exterior orientation parameters, including orbital and attitude, are characterized by second order polynomials as functions of sampling time t relative to the first scan line,

$$\begin{aligned} x_i &= -f\frac{m_{11t}(X_i - X_t^c) + m_{12t}(Y_i - Y_t^c) + m_{13t}(Z_i - Z_t^c)}{m_{31t}(X_i - X_t^c) + m_{32t}(Y_i - Y_t^c) + m_{33t}(Z_i - Z_t^c)} \\ S_y \cdot y_i &= -f\frac{m_{21t}(X_i - X_t^c) + m_{22t}(Y_i - Y_t^c) + m_{23t}(Z_i - Z_t^c)}{m_{31t}(X_i - X_t^c) + m_{32t}(Y_i - Y_t^c) + m_{33t}(Z_i - Z_t^c)} \end{aligned} \tag{4}$$

where,

x ,y are the photo coordinates,

X, Y, Z are the object coordinates,

X_t^c, Y_t^c, Z_t^c are the exterior orbital parameters, and

m_{11t}, m_{12t}, .. m_{33t} are the rotation matrix,

The purpose of the least squares adjustment in this investigation is to determine the most probable values for the ground coordinates of all the unknown points and the exterior orientation parameters of all images. Besides the collinearity equations, exterior orientation parameters and object coordinate are included in the observation equations. We can correct exterior orientation parameters, ground coordinates of GCPs and tie points when a priori error is assumed. Then, we formulate weight of all parameters to distinguish the high correlation between location and attitude, and the difference between GCPs and tie points, as shown in equation 5.

$$\begin{aligned} &\dot{V}_{ij} + \dot{B}_{ij}\dot{\Delta}_i + \ddot{B}_{ij}\ddot{\Delta}_j = \varepsilon_{ij} && \textit{Collinearity Equations} \\ &\dot{V}_i - \dot{\Delta}_i = \dot{C}_i && \textit{Exterior Orientation Parameters} \\ &\ddot{V}_j - \ddot{\Delta}_j = \ddot{C}_j && \textit{Ground Control Equations} \end{aligned} \tag{5}$$

Where,

$\dot{\Delta}_i$ is the correction of exterior orientation parameters,

$\ddot{\Delta}_j$ is the correction of ground coordinates,

$\dot{B}_{ij}, \ddot{B}_{ij}$ are the partial derivatives,

$\dot{C}_i$, $\ddot{C}_j$ are the approximation of measurement, and

ε_{ij} is the measured image coordinates.

In order to overcome the weak geometry for tie points, we use DEM in the adjustment for elevation control. First, ray tracing technique is applied to determine the ground position of a tie point. The result locations of different orbits for the same tie points are not coincident. We take the average position of two ground points as the initial position of this tie point. Figure 3 illustrates the work flow of DEM elevation control.

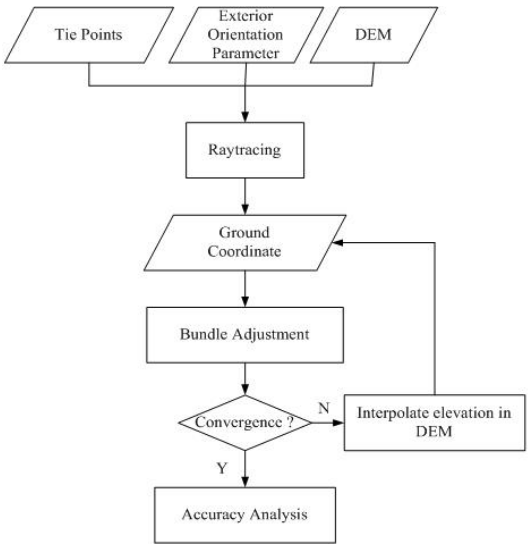

Figure 3. Work Flow of elevation control

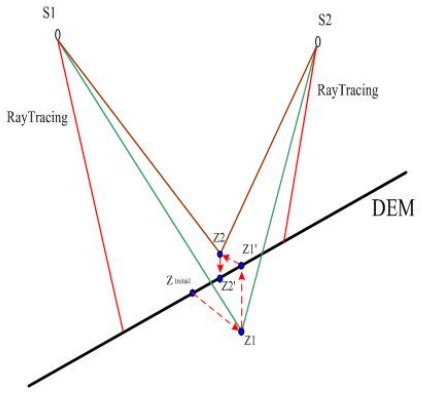

Figure 4. Illustration of DEM elevation control

Because the weak geometry of intersection exhibits elevation errors, we strive to use DEM recursively in the least squares adjustment. Referring to Figure 4, the elevation "Z" without "prime" denotes the elevation after bundle adjustment, and the "Z" with "prime" denotes the elevation after interpolation in DEM. The subscripts of Z mean the number of iterations. The computation procedure starts from the initial value of Z1 to Z1', then to Z2 and Z2', and so forth until converged. In this way, we can control elevation error in a reasonable range that the convergence is expected.

2.3 Rational Function Model

The proposed method comprises two parts too. The first one is RFM-based block adjustment. The second one is elevation control with DEM.

The RFM uses the ratio of two cubic polynomials and the RPCs that are determined by fitting the physical camera model to describe the relationship between object space and image space. In order to maintain the numerical precision, object and image space coordinates will be normalized to (-1, +1). General forms of RFM can be written as equation 6.

$$x = \frac{p_a(X,Y,Z)}{p_b(X,Y,Z)} = \frac{\sum_{i=0}^{m1}\sum_{j=0}^{m2}\sum_{k=0}^{m3} a_{ijk} X^i Y^j Z^K}{\sum_{i=0}^{n1}\sum_{j=0}^{n2}\sum_{k=0}^{n3} b_{ijk} X^i Y^j Z^K}$$
$$y = \frac{p_c(X,Y,Z)}{p_d(X,Y,Z)} = \frac{\sum_{i=0}^{m1}\sum_{j=0}^{m2}\sum_{k=0}^{m3} c_{ijk} X^i Y^j Z^K}{\sum_{i=0}^{n1}\sum_{j=0}^{n2}\sum_{k=0}^{n3} d_{ijk} X^i Y^j Z^K} \quad (6)$$

Where,
x, y are the image coordinates,
X, Y, Z are the object coordinates, and
a_{ijk}, b_{ijk}, c_{ijk}, d_{ijk}, are the polynomial coefficients.

The coefficients of the RFM are called rational polynomial coefficients (RPCs). Typically, as the RPCs are selected to the third degree, eighty coefficients are essentially included. There are two approaches to determine the RPCs. The first one is GCP-derived RPC which employs numerous GCPs to derive the coefficients. However, as this approach requires too many GCPs, it is considered unrealistic. The second one is sensor-oriented RPC which utilizes the satellite on-board orientation includes orbital parameters and attitude data in generating enough transformation anchor points. This method achieves a high precision under the circumstances that the on-board orbital parameters and attitude data are accurate. As most high resolution satellites are equipped with instruments such as GPS, INS, and star trackers, they are capable of providing satisfactory orientation measurements. Accordingly, the sensor-oriented RPC is selected in this investigation.

In order to compensate the systematic bias of RPCs, we use an affine transformation to correct the error in the image space. The affine transformation coefficients can be calculated from ground control points. The equation of affine transformation is shown as equation 7.

$$S_{GCP} = p_0 + p_1 \cdot S_{RFM} + p_2 \cdot L_{RFM}$$
$$L_{GCP} = q_0 + q_1 \cdot S_{RFM} + q_2 \cdot L_{RFM} \quad (7)$$

Where,
(S_{GCP}, L_{GCP}) are the image coordinates of GCP,
(S_{RFM}, L_{RFM}) are the image coordinates determined by RFM,
p_0~q_2 are the affine coefficients.

Block adjustment could enhance the geometry consistency between the images to reach high accuracy for orientation determination. The observation equation of RFM and object coordinate are included in the block adjustment. Since the affine coefficients are not highly correlated, we only consider the object coordinate rather than the extra observation equation of affine coefficients. The observation equations are shown in equation 8.

$$V_{ij} + \dot{B}_{ij}\dot{\Delta}_i + \ddot{B}_{ij}\ddot{\Delta}_j = \varepsilon_{ij}$$
$$\dot{V}_i - \dot{\Delta}_i = \dot{C}_i \quad (8)$$

Where,
$\dot{\Delta}_i$ is the correction of affine coefficients,
$\ddot{\Delta}_j$ is the correction of ground coordinates,
$\dot{B}_{ij}, \ddot{B}_{ij}$ are the partial derivatives,
$\dot{C}_i$ is the approximation of measurement, and
ε_{ij} is the measured image coordinates.

Due to the weakly convergent, a DEM is included in the block adjustment as an elevation control in this investigation. The idea of this elevation control is same as the procedure of modified bundle adjustment. Firstly, we use the new (X, Y) in each iteration of block adjustment to interpolate a new Z in the DEM. It will get an accurate result through iteration and interpolation to overcome the problem of elevation error.

3. EXPERIMENTAL RESULTS

The test data include three strips of SPOT 5 supermode panchromatic images. The test area is in the middle part of Taiwan from west coast to east coast as shown in Figure 5. Those strips are with about 10% overlap as shown in Figure 6. The ground control points and independent check points (ICPs) are acquired from 1:5000 scale topographic. The tie points (TP) and independent check tie points (ICTP) are acquired by manual measurements. It covers an area with 3800m terrain relief. Related information of the test images is shown in Table 1. The experiments include three parts of validation. The first one is to evaluate the geometrical consistency between strips. The second one is to examine the absolute accuracy. The last part is to check the mosaic image. In this section, the "Direct Georeferencing", "Modified Bundle Adjustment" and "Rational Function Model" are noted as **DG**, **MBA**, and **RFM**, respectively. The 80 RPCs for each of the images are generated according to Chen et al., (2006).

	Strip1	**Strip2**	**Strip3**
GSD	2.5m		
Image Size	24000*24000		

Date	2003/6/21	2003/5/31	2003/7/1
Incidence Angle	5.21	5.65	-14.76
Number of GCP	9	9	9
Number of ICP	25	12	12
Number of TP	30	24	
Number of CTP	18	13	
DEM	40m Topographic Data Base of Taiwan		
Elevation Range	1~3700m		

Table 1. Related information of test data

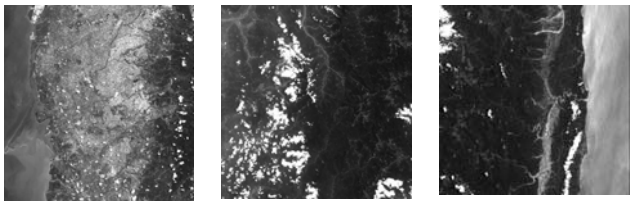

(a) (b) (c)

Figure 5. Test images: (a) strip 1, (b) strip 2, (c) strip 3.

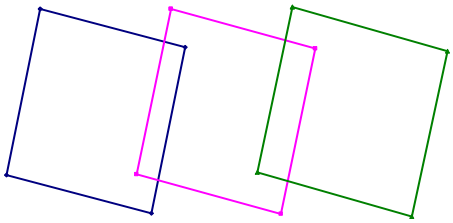

Figure 6. Overlapping area of the test images

3.1 Geometrical Consistency between Strips

A pair of tie points will appear in two images. We thus check ground positions of tie point using independent check tie points. Distance between these two ground positions is used to evaluate the discrepancy. Table 2 illustrates the accuracy performance of independent check tie points in the independent adjustment. Table 3 shows the accuracy performance of independent check tie points in the independent adjustment. For strip 1 and 2, the RMSE of ICTP before the block adjustment is around 11.6m and 8.7m. After the block adjustment, the RMSE of ICTP is improved to 2.0m and 1.7m in E and N directions. For strips 2 and 3, the improved of ICTP RMSE is from 29.9m and 30.0m to 4.4m and 5.2m in E and N directions, respectively. Significant improvement of geometrical consistency is demonstrated when tie points are employed in the block adjustment. The difference of these three methods is less than 1m (i.e. 0.4 pixels) for all strips in block adjustment.

Unit: meter	**Strip 1 &2**		**Strip2 & 3**	
	No. ICTP = 18		**No. ICTP = 13**	
DG	**RMSE E**	**RMSE N**	**RMSE E**	**RMSE N**
ICTP	10.88	7.09	29.89	30.03
MBA	**RMSE E**	**RMSE N**	**RMSE E**	**RMSE N**
ICTP	11.56	8.72	28.37	25.01
RFM	**RMSE E**	**RMSE N**	**RMSE E**	**RMSE N**
ICTP	8.21	7.17	24.99	29.50

Table 2. Comparison of geometrical consistency without block adjustment

Unit: meter	**Strip 1 &2**		**Strip2 & 3**	
	No. TP = 19 **No. ICTP = 18**		**No. TP = 13** **No. ICTP = 13**	
DG	**RMSE E**	**RMSE N**	**RMSE E**	**RMSE N**
TP	1.62	1.21	5.07	4.35
ICTP	2.04	1.31	3.04	4.94
MBA	**RMSE E**	**RMSE N**	**RMSE E**	**RMSE N**
TP	2.17	1.27	5.27	3.61
ICTP	1.22	1.68	3.56	4.24
RFM	**RMSE E**	**RMSE N**	**RMSE E**	**RMSE N**
TP	0.90	0.44	2.08	2.53
ICTP	1.06	1.15	4.35	5.18

Table 3. Comparison of geometrical consistency with block adjustment

3.2 Absolute Accuracy

The absolute accuracy is evaluated by the independent check points. This test includes the comparison of three proposed block adjustment method. Furthermore, the result of independent adjustment is also provided for comparison. Table 4 shows the independent adjustment results of the three proposed method. The number of GCP and ICP are also indicated in the corresponding table. The result of strip 3 is around 8m because the view angle is about 15 degree and the high terrain relief. The absolute accuracy of strip 1 is better than strip 2 because of the terrain relief of strip 1 is lower than strip 2. The difference of these three methods is less than 1.25m (i.e. 0.5 pixels) for all strips.

Unit: meter	**Strip1** **No. GCP= 9** **No. ICP = 25**		**Strip2** **No. GCP= 9** **No. ICP = 12**		**Strip3** **No. GCP= 9** **No. ICP = 12**	
DG	**RMSE E**	**RMSE N**	**RMSE E**	**RMSE N**	**RMSE E**	**RMSE N**
GCP	2.52	1.26	2.71	2.11	1.70	3.32
ICP	4.76	2.61	2.78	5.55	6.48	7.80
MBA	**RMSE E**	**RMSE N**	**RMSE E**	**RMSE N**	**RMSE E**	**RMSE N**
GCP	2.41	1.10	2.27	0.81	1.05	2.26
ICP	4.01	3.01	3.05	5.99	5.69	6.65
RFM	**RMSE E**	**RMSE N**	**RMSE E**	**RMSE N**	**RMSE E**	**RMSE N**
GCP	3.78	1.86	3.10	2.54	2.46	3.95
ICP	3.77	2.64	2.54	6.12	5.76	7.37

Table 4. Comparison of absolute accuracy without block adjustment

Table 5 provides the results of block adjustment. The initial parameters for block adjustment are calculated from independent adjustment. Moreover, a DEM is applied to overcome the weak geometric. The result of these three block adjustment methods is quite consistent except RFM in strip 3. The absolute accuracy of independent adjustment is not better than block adjustment. It is because the block adjustment should satisfy the GCP and TP in the block. The absolute accuracy of these three strips are from 2.2m to 8.8m.

Unit: meter	Strip1 No. GCP= 9 No. ICP = 25 No. TP = 19		Strip2 No. GCP= 9 No. ICP = 12 No. TP = 32		Strip3 No. GCP= 9 No. ICP = 12 No. TP = 13	
DG	**RMSE E**	**RMSE N**	**RMSE E**	**RMSE N**	**RMSE E**	**RMSE N**
GCP	4.51	3.24	8.43	8.70	5.94	3.33
ICP	4.89	2.27	7.43	8.75	5.64	3.65
MBA	**RMSE E**	**RMSE N**	**RMSE E**	**RMSE N**	**RMSE E**	**RMSE N**
GCP	3.29	1.60	4.49	2.98	4.91	5.19
ICP	4.92	3.57	6.33	8.81	5.46	3.56
RFM	**RMSE E**	**RMSE N**	**RMSE E**	**RMSE N**	**RMSE E**	**RMSE N**
GCP	4.18	2.52	4.40	3.75	5.28	4.86
ICP	4.05	2.55	5.83	8.13	4.90	6.83

Table 5. Comparison of absolute accuracy with block adjustment

3.3 Summary

The experimental results are summarized as follows.

(1) The geometric performances for the three proposed methods are similar.
(2) The proposed methods significantly improve the geometric consistency between overlapping images with respect to the individual adjustment. The improvements are about a factor of 5.
(3) The RMSE of independent check points slightly increase when a block adjustment is employed.
(4) It is expected that the DEM in the extremely hilly mountain areas is less accurate than the GCPs and ICPs. That could explain why the geometric consistency improves while the RMSE of check points deteriorates. Nevertheless, the payoff reveals the effectiveness of the block adjustment.

3.4 Mosaic Images

Since, the performance of three methods provides promising and consistent results. We select the modified bundle adjustment method to show the geometrical consistency in the image space. The generated mosaics image from those three images is shown in Figure 7. We also compare the mosaicking results of independent and block adjustment. There are two sample enlargements as shown in Figure 8 for a comparison. In figure 8a, we find obvious discontinuity along the seam line. This condition is significantly improved in figure 8b. Figure 8c and 8d also show that the block adjustment may improve the geometrical consistence.

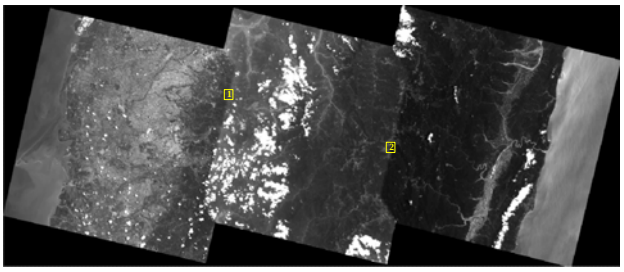

Figure 7. Mosaic image by block adjustment without grey value balance

4. CONCLUSIONS

In this research, we compare three approaches of block adjustment methods for satellite images with weak convergent geometry by using DEM as an elevation control. The first one is a revised version of traditional bundle adjustment. The second one is based on the direct georeferencing approach. The third one is a rational function model with sensor-oriented rational polynomial coefficients. The experimental results indicate that the proposed method using DEM as elevation control could significantly improve the geometric accuracy as well as the geometric discrepancies. These three block adjustment methods provide consistent results. After comprehensive tests, it is indicated that the proposed method has a good chance in real applications. The satellite ground receiving station of Taiwan, located in National Central University, just began to integrate the scheme in the orthorectification for multiple satellite images as daily operation.

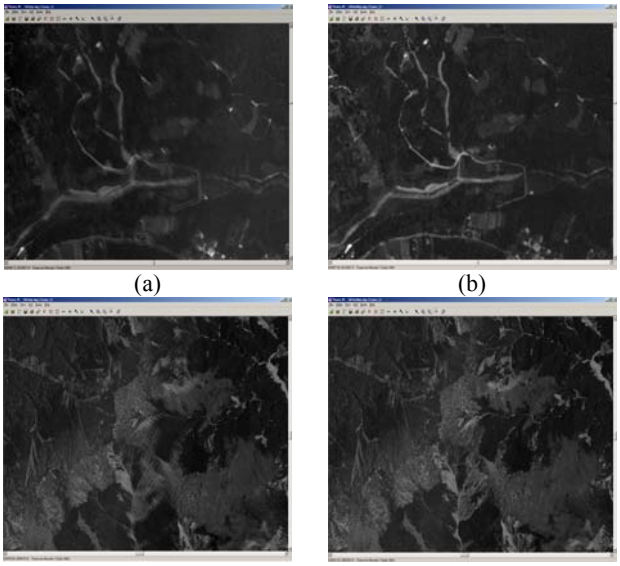

(a) (b) (c) (d)

Figure 8. Comparison of independent and block adjustment by mosaic image: (a) results of independent adjustment in area 1, (b) results of block adjustment in area 1, (c) results of independent adjustment in area 2, (d) results of block adjustment in area 2.

ACKNOWLEDGEMENTS

This investigation was partially supported by the National Land Surveying and Mapping Center of Taiwan under Project No. LSB-96-47.

REFERENCES

Chen, L.C., and Lee, L.H. 1993. Rigorous Generation of Digital Orthophoto from SPOT Images. Photogrammetric Engineering and Remote Sensing, 59(5): 655-661.

Chen, L. C., Teo, T. A., and Liu, J. L., 2006. The Geometrical Comparisons of RSM and RFM for FORMOSAT-2 Satellite Images, Photogrammetric Engineering and Remote Sensing. 72(5): 573-579.

Dowman, I.J., and Michalis, P., 2003. Generic rigorous model for along track stereo satellite sensors, ISPRS Workshop on

high resolution mapping from space. 6-8 October, 2003, Hanover. (on CD-ROM).

Fraser, C.S., Dial, G., and Grodecki, J., 2006. Sensor orientation via RPCs, ISPRS Journal of Photogrammetry and Remote Sensing, 60(3): 182-194.

Grodecki, J. and Dial, G., 2003, Block Adjustment of High-Resolution Satellite Image Described by Rational Function, Photogrammetric Engineering and Remote Sensing, 69(1): 59-68.

Mikhail, E.M. and Ackermann, F., 1982, Observation and Least Squares, University Press of America, New York, pp 393-426.

Orun, A.B. and Natarajan, K., 1994. A modified bundle adjustment software for SPOT imagery and photogrammetry: tradeoff. Photogrammetric Engineering and Remote Sensing, 60(12): 1431-1437.

Poli, D., Zhang, L. and Gruen, A., 2004. Orientation of satellite and airborne imagery from multi-line pushbroom sensors with a rigorous sensor model. International Archives of Photogrammetry and Remote Sensing, 35(B1): 130-135.

Toutin, Th., 2003, Block Bundle Adjustment of IKONOS In-Track Image, International Journal of Remote Sensing, 24(4):851-857.

Westin, T., 1990. Precision rectification of SPOT imagery, Photogrammetric Engineering and Remote Sensing, 56(2): 247-253.